Eur Biophys J (2006) 35: 424–430
DOI 10.1007/s00249-006-0049-7

ARTICLE

Borys Kierdaszuk · Jakub Włodarczyk

Interpretation of intramolecular stacking effect on the fluorescence intensity decay of 3-methylbenzimidazolyl(5′-5′)guanosine dinucleotides using a model of lifetime distribution

Received: 12 October 2005 / Revised: 20 January 2006 / Accepted: 7 February 2006 / Published online: 3 March 2006

Abstract Time-resolved fluorescence of 3-methylbenzimidazole (m^3B) was used to study stacking interaction between base moieties in di-, tri- and tetra-phosphate analogues of 3-methylbenzimidazolyl(5′-5′)guanosine (m^3Bp_nG, n = 2, 3, 4), using 5′-triphosphate of 3-methylbenzimidazole riboside (m^3BTP) as reference. Fluorescence intensity decays of all compounds cannot be satisfactory fitted with single-exponential function. Although an increase of a number of exponents led to better fits, interpretation of the individual exponential terms, i.e. pre-exponential amplitudes and fluorescence lifetimes, cannot be adequately characterized. We show that these fluorescence decays are best fitted by power-like function derived from physically justified distribution of the fluorescence lifetimes, and characterized by the mean value of the excited-state lifetime and relative variance of lifetime fluctuations around the mean value. The latter led to the parameter of heterogeneity and number of decay paths, which depend on the factors responsible for non-radiative decay of the excited state, including base–base stacking interaction. This was studied by means of changes of temperature and the number of phosphate groups in dinucleotides. It was shown that the strongest effect of stacking interactions, characterized by lowest values of both fluorescence mean decay time and relative variance, occurs in the case of m^3Bp_3G containing the same number of phosphates as natural mRNA cap. The possible importance of these results for interpretation of the mechanism of function of the mRNA cap structure is discussed.

Keywords Non-exponential fluorescence decay · Lifetime distribution · q-Exponential function · Base–base stacking interaction

B. Kierdaszuk (✉) · J. Włodarczyk
Department of Biophysics, Institute of Experimental Physics, University of Warsaw, 93 Zwirki i Wigury St., 02-089, Warsaw, Poland
E-mail: borys@biogeo.uw.edu.pl
Fax: +48-22-5540771

Abbreviations m^3B: 3-Methylbenzimidazole · G: Guanine · m^3BR: 3-Methylbenzimidazole-1-β-D-ribofuranoside · m^3BTP: 3-Methylbenzimidazole-1-β-D-ribofuranoside 5′-triphosphate · m^3Bp_nG (n = 2, 3 and 4): Di-, tri- and tetra-phosphate 3-methylbenzimidazolyl(5′-5′)guanosine · m^7G: 7-Methylguanine · eIF4E: Eukaryotic initiation factor

Introduction

Non-specific stacking interactions between nucleic acid bases involve a number of intermolecular forces, such as dipol–multipole (dipole–dipole, dipole–quadrupole), dipol-induced dipole, charge transfer, as well as induction and dispersion forces. The best-known example is the stacking interactions between nucleic acid bases in DNA/RNA chains which are, besides the lateral hydrogen bonding (base pairing), responsible for stability and conformational arrangement of nucleic acids. They also play a key role in determining the structure and dynamics of various complexes of these biomacromolecules with intercalators and minor or major grove binders (Saenger 1984) including proteins.

One of the most interesting example of stacking interactions occur in the mRNA-cap complex with cap-binding proteins (e.g. translation initiation factors) in the ribosomal assembly. Interaction of eukaryotic initiation factor 4E (eIF4E) with $m^7G(5')ppp(5')N$ (where N is any nucleotide) cap structure at the 5′ terminus of mRNA is a fundamental event of the translation initiation (Mathews et al. 2000). This is achieved almost entirely by the interactions of m^7G with two aromatic residues (Trp56 and Trp102) in cation-π sandwich (Hu et al. 2003). As was concluded from 3D structures of mouse and human eIF4E bound to mono- and dinucleotide cap analogues (Marcotrigiano et al. 1997; Tomoo et al. 2002, 2003), and from fluorescence titration (Niedzwiecka et al. 2002) and stopped-flow studies

(Blachut-Okrasinska et al. 2000; Dlugosz et al. 2003), electrostatic interactions are crucial for recognition of cap structure by eIF4E. It was proposed that the negatively charged cap phosphate chain might play a role of a molecular anchor at the beginning of binding of eIF4E protein (Niedzwiecka et al. 2002).

At the next step, sandwich-type stacking interactions between the positively charged m^7G and the side chains of two tryptophan residues (Trp56 and Trp102), supported by three hydrogen bonds between the protein and m^7G, play a stabilizing role for this complex. Therefore, clarification of the role of stacking interactions in the mechanism of cap recognition and binding may help to understand the mechanism of translation initiation, and may lead to more rational design of cap analogue inhibitors with potential pharmacological applications.

Stacking interactions between tryptophan residues of the eIF4E protein and m^7G are competitive with intramolecular stacking interaction between m^7G and a second base of the cap. The latter was previously described for several cap analogues by temperature-dependent association constants, enthalpy and entropy for equilibrium between stacked and unstacked base moieties in dinucleotides using steady-state fluorescence, and time-resolved fluorescence intensity decays analysed with multiexponential models (Wieczorek et al. 1997). The number of exponential terms was affected by temperature. Fluorescence decays at high temperature (~70°C) were roughly described by single-exponential function. Decreasing temperature led to an increase in the number of exponents, and at least three-exponential function was needed at 5°C, where equilibrium was shifted towards the stacked form of dinucleotides. Although increasing number of exponents improved those fits, their physical interpretation was unknown. Observed components are not due to spectral shifts, because vibrational and solvent relaxation occurs on a subpicosecond timescale in the dinucleotides (Larsen et al. 2004), and the position and shapes of the steady-state fluorescence spectra are very similar for different dinucleotides studied here, and are not changed with temperature (data not shown). This was further supported by the time-resolved fluorescence of m^3BTP, used here as a reference. Thus, temperature-dependent heterogeneity of the excited state decays in dinucleotides is due to their excited-state dynamics. The latter was thoroughly investigated with the aid of 2-aminopurine, fluorescent analogue of adenine, which was used as a fluorescence probe of interactions between neighbouring bases, e.g. conformational transitions (O'Neill et al. 2003a, b), base flipping (Su et al. 2004), unstacking (Jean and Hall 2004) and electron transfer (O'Neill and Barton 2004).

All the foregoing discussion shows that oligonucleotides are complex systems constituted by equilibrium of many energetic states with time-dependent interconversions between them. Therefore, we have analysed for the first time fluorescence decays of dinucleotide analogues of the cap using fluorescence lifetime distribution and power-like decay function (Eq. 2), which is an example of application of q-exponential function originally introduced by Tsallis (1988). This function, resulted from a model of continuous lifetime distribution around the mean value of excited-state lifetime, was previously applied for the protein (enzyme and enzyme–ligand) systems (Wlodarczyk and Kierdaszuk 2003). It turned out that this approach led not only to new observations regarding applicability of the fluorescence lifetime distribution and power-like function for analysis of oligonucleotide fluorescence decays, but also exhibited some unusual properties of the mRNA cap, which we now describe.

Materials and methods

Materials

3-Methylbenzimidazole (m^3B) analogues of dinucleoside polyphosphates (m^3Bp_nG, n = 2, 3, 4) and 5′-triphosphate of 3-methylbenzimidazole riboside (m^3BTP) were synthesized as described (Chlebicka et al. 1995). Tris–HCl buffer (pH 7.5) was made using tris-(hydroxymethyl)-aminomethane hydrochloride (Merck, Darmstadt, Germany), HCl (Aldrich) and MilliQ water (Millipore, Austria).

Methods

Fluorescence intensity decays were measured using a picosecond time-correlated single-photon counting fluorometer. The source of excitation light was obtained by pumping Mira 900 Ti:Sapphire laser with Innova 310 argon ion laser (both from Coherent, Santa Clara, USA), 8 W at 530 nm, CW. Excitation was accomplished at 285 nm using the horizontally polarized fundamental output of a cavity-dumped Ti:Sapphire laser at 855 nm and 76-MHz repetition rate, which was passed through a 9200 pulse selector (Coherent, USA) reducing repetition rate to 4.75 MHz, and a 5-050 frequency tripler (Inrad, NJ, USA). In order to improve polarization of the excitation beam, it was passed through a Glan-Thompson vertical polarizer, and focused on a sample using a 5-cm focal length lens. The time between exciting pulses was at least 10-fold longer than the measured lifetime, ensuring excitation of a fully equilibrated sample with each laser pulse. Fluorescence detection was based on MCP-PMT Hammamatsu detector, thermoelectrically cooled, and set up in the time-correlated single photon counting mode. The overall system response time was 60 ps FWHM of the IRF. We used 1.0×1.0 cm^2 cuvettes placed in the thermostated cell holder, with a focal point positioned about 0.5 cm from the surface facing incident light. The position of the cuvette and lens was adjusted so that the focal point of the laser excitation was located near the observation window. Fluorescence was collected by suprasil lens, filtered from the contaminating excitation

using a Corning 345-nm long-wavelength-pass filter, and passed Glan-Thompson polarizer set at the magic angle (54.7°) relative to excitation polarization. All measurements were performed at a concentration of 5 μM of m^3Bp_nG (n = 2, 3, 4) and m^3BTP, where inner filter effect and intermolecular stacking association may be neglected. Signal from the solvent alone was less then 0.5% and was subtracted from sample fluorescence.

Assumed decay functions in the form of one-, two- or three-exponential function (Eq. 1), and power-like function (Eq. 2) were iteratively convoluted with the instrument response function, and results were compared with measured fluorescence decays using IBH time-domain software (IBH Consultants, Glasgow, UK) and homemade procedures under Matlab, respectively. Non-linear fitting procedure, in the form of the Marquardt–Levenberg method (Marquardt 1963; Levenberg 1944), was applied. The quality of fits was evaluated by the structure observed in the plots of residual differences between experimental (I_{exp}) and theoretical (I_{teo}) values normalized to errors, i.e. $(I_{exp} - I_{teo})/\sqrt{(I_{exp} + I_{teo})}$, representing deviations between measured and calculated data (Fig. 1, bottom panels), and by the reduced chi-square (χ^2_R) values.

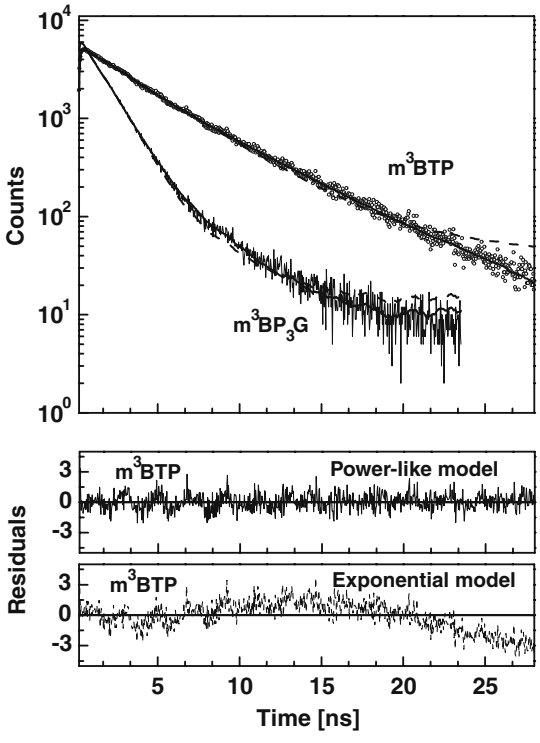

Fig. 1 Comparison of the theoretical values of the best fits of power-like function (*solid lines*) and monoexponential function (*dashed lines*) to the fluorescence intensity decays (*dotted curves*) of 5 μM m^3BTP and m^3Bp_3G in 20 mM Tris–HCl buffer (pH 7.5) at 40°C. Note the difference between the reduced chi-square (χ^2_R) values: 0.92 (m^3BTP) and 1.3 (m^3Bp_3G), and 6.7 (m^3BTP) and 2.6 (m^3Bp_3G) for fits of the power-like function and monoexponential function, respectively. The *lower panels* show the residual differences between experimental (I_{exp}) and theoretical (I_{teo}) values normalized to errors, i.e. $(I_{exp} - I_{teo})/\sqrt{(I_{exp} + I_{teo})}$

Theory

In the classical analysis of fluorescence decay (multiexponential model), intensity decays $I(t)$ are fitted using

$$I(t) = \sum_i \alpha_i \exp\left(-\frac{t}{\tau_i}\right) \quad (1)$$

where α_i are the amplitudes associated with the decay time values τ_i. The mean decay time $\langle\tau\rangle$ is given by $\langle\tau\rangle = \sum_j f_j\tau_j$, where fractional intensity decay f_j is given by $f_j = \alpha_j\tau_j/\sum_i \alpha_i\tau_i$. Multiexponential model of fluorescence decays is usually applied for a homogenous system of fluorophores. However, this is not the case of studied system. Occurrence of stacking interaction implies dynamical quenching mechanism of fluorescence, the rates of which compete with the rate of the fluorescence emission. Furthermore, such fluorescence quenching (excitation transfer) lead to a hierarchy of time scales in considered system. This in turn, as was shown previously for protein fluorescence decay (Wlodarczyk and Kierdaszuk 2005), may be represented as a distribution of lifetimes. In this case, the total decay rate $\gamma = 1/\tau$ is expected to be a sum of a number (N) of partial rates γ_i ($\gamma = \sum_{i=1}^{N} \gamma_i$). The consequence of assuming that the total rate is a composition of many partial rates leads to its distribution in the form of gamma distribution (Wlodarczyk and Kierdaszuk 2003), which is the most probable under experimental constraints. The number N of partial decay rates (γ_i) represents a combination of all internal states of the system, and is called the number of decay channel, because it reflects a set of energetically discriminated configurations of the system long before and long after the decay takes place.

In the case of base–base stacking in dinucleotides studied here we use the power-like decay function (Eq. 2) resulted from gamma distributed fluctuations of fluorescence decay rates γ

$$P_N(\gamma)d\gamma = \frac{1}{\Gamma\left(\frac{N}{2}\right)}\left(\frac{N}{2\langle\gamma\rangle}\right)\left(\frac{N\gamma}{2\langle\gamma\rangle}\right)^{(N/2)-1}\exp\left(-\frac{N\gamma}{2\langle\gamma\rangle}\right)$$

The power-like decay function was previously applied for analysis of protein fluorescence decays (Wlodarczyk and Kierdaszuk 2003) in the form

$$I(t) = A\left[1 - (1-q)\frac{t}{\tau_0}\right]^{1/(1-q)} \quad (2)$$

where A is the amplitude, τ_0 is the mean value of lifetime distribution and q is the parameter of heterogeneity defined as

$$q = 1 + \frac{2}{N} = 1 + \frac{\left\langle(\gamma - \langle\gamma\rangle)^2\right\rangle}{\langle\gamma\rangle^2} = 1 + \omega \quad (3)$$

describing the number of decay channels (N) and relative variance (ω) of fluctuations of $\gamma = 1/\tau$ around the $1/\tau_0$

value (Wilk and Wlodarczyk 1999). The mean decay time $\langle \tau_p \rangle$ is given by

$$\langle \tau_p \rangle = \frac{\tau_0}{3 - 2q} \quad (4)$$

It is worth noticing that in the limit, when the number of decay channels goes to infinity, i.e. $q \rightarrow 1$, the decay function from a power-like form (Eq. 1) converges to a single-exponential form (Tsallis 1988).

Results and discussion

Fluorescence emission properties of m^3B analogues

It should be noted that, at physiological pH, m^7G consists of an equilibrium mixture of cationic and zwitterionic forms, with pK_a value of 7 (Stoychev et al. 2001) for dissociation of the purine ring N(1)–H. Since m^7G is weakly fluorescent (quantum yield $\Phi \sim 1$ and 0.4% for the cationic and zwitterionic forms, respectively), and fluorescence intensity decay of m^7G occurs in the picosecond time scale (Wieczorek et al. 1997), it is not a suitable fluorescence probe for local dynamic of oligonucleotides and nucleic acids. Therefore, m^7G in the cap analogues was replaced by 3-methylbenzimidazole (m^3B, Scheme 1), which exists in the chemically fixed cationic form, and is used here as a close structural analogue of the cationic form of m^7G. All m^3B, m^3BR and m^3BTP are strongly fluorescent ($\Phi \sim 30\%$), but in the cap analogues, m^3B fluorescence (λ_{max} 370 nm) is 10-fold quenched as a result of base stacking. This is in line with an almost 10-fold increase in fluorescence emission due to enzymatic cleavage of the oligophosphate bridge in m^3Bp_3G, used as a highly sensitive method for following the kinetics of the reactions (Chlebicka et al. 1995). Strong stacking interaction between the m^3B and the neighbour G moiety has been also shown recently (Dlugosz and Wlodarczyk 2004) by molecular dynamic simulations of m^3BP_3G in water using CHARMM package (Brooks et al. 1983). The minimal distance between parallel planes of the bases was about 3.7 Å similar to that of stacking association between m^7G and G (Stolarski et al. 1996). Thus, m^3B may be used here as a probe of stacking interactions between neighbouring bases. Fluorescence intensity of m^3B decays in the nanosecond range and enables detection of the effect of cation-π stacking interaction on the parameters of power-like function.

Power-like model

Fluorescence intensity decays of m^3BTP and m^3Bp_nG (n = 2, 3 and 4) are highly non-exponential (see examples in Fig. 1) with a temperature-dependent number of exponential terms needed for satisfactory fits (data not shown). Unfortunately, two-exponential model, based on the assumption that exponential terms represent fluorescence decay of the stacked and unstacked forms of dinucleotides, and relative values of fractional intensity factors quantitatively reflect a shift of the temperature-dependent equilibrium between them, also exhibited bad fit ($\chi^2_R \sim 2$) of fluorescence decays of the m^3Bp_nG (n = 2, 3 and 4) at low temperatures. Further improvement of the goodness of fit was obtained by addition of the third-exponential term (data not shown), but without its physical justification.

Therefore, we have made a search for alternative model assuming that fluorescence decay is affected by a continuous relaxation of the system. Consequently, classical model of discrete components (sum of the exponential terms) was replaced by continuous lifetime distribution model in the form of gamma distribution of the decay rates similar to that of protein fluorescence (Wlodarczyk and Kierdaszuk 2003). These led to the power-like function (Eq. 2), which characterize fluorescence intensity decays by the mean value (τ_0) of fluorescence lifetime distribution and relative variance of distribution (ω) (Eq. 3). Figure 1 presents examples of the comparison of typical fits of single exponent and power-like function to fluorescence decays of m^3BTP and m^3Bp_3G at 40°C. Fittings of the power-like function (Fig. 1, middle panel) led to random deviations of the residuals normalized to error, indicating that the only source of difference is the random error in the data. The randomness of the deviations indicates that this model is adequate to explain the data, and estimated parameter values have the highest probability of being correct. In contrast, deviations for the one-exponential fit (Fig. 1, bottom panel), as well as for two- and three-exponential

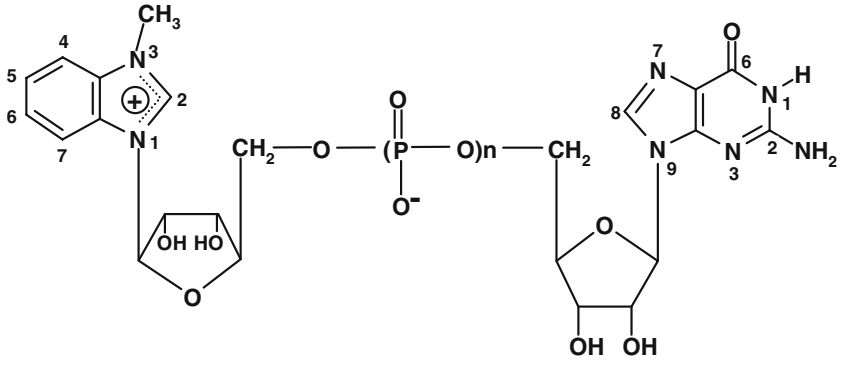

Scheme 1 Di-, tri- and tetra polyphosphate analogues of 3-methylbenzimidazolyl(5′-5′)guanosine dinucleotides (m^3Bp_nG, n = 2, 3, 4) containing neutral form of guanosine (pK_a 9.3). Note the cationic form of m^3B

fits (data not shown) are not random, and indicate that these models are not adequate. The latter is also reflected in the χ^2_R values, which are approaching 1 for power-like function, and are generally much higher for one-exponential fits. As is seen from the normalized residuals and the reduced chi-square (χ^2_R) values, there is no doubt that power-like formula significantly improved the analysis and fits fluorescence decays much better, especially in the tail of the decay profiles.

All the foregoing discussions suggest that the heterogeneity parameter (q) values derived from the variance of fluorescence lifetime distribution (Eq. 3) objectively characterize heterogeneity of the oligonucleotide analogues of the cap. Properties of the cap oligonucleotides are also reflected in the fluorescence decay kinetics described by the mean decay time $\langle\tau_p\rangle$ values. They both are physically justified and provide new information about studied system (see Temperature effect on the fluorescence intensity decays section).

Temperature effect on the fluorescence intensity decays

The effects of temperature on the m^3G fluorescence intensity decay in dinucleotide cap-analogues were studied in the range of 5–75°C, where dinucleotides consist of an equilibrium mixture of the stacked and unstacked forms due to intramolecular base–base stacking (Wieczorek et al. 1997; Nishimura et al. 1980). The fluorescence lifetime values observed here are of the order of a few ns, hence fluorescence decay kinetics may be affected by intramolecular base–base stacking of dinucleotides.

The mean decay time ($\langle\tau_p\rangle$) (Eq. 4) and parameter of heterogeneity (q) values were used to describe fluorescence decay kinetics. They were obtained from non-linear least-square fittings of the power-like function (Eq. 2) to fluorescence intensity decays of 5 μM m^3BTP and m^3BR-guanosine dinucleotide. Results of fittings are shown in Fig. 2. For m^3BTP at this concentration, where intermolecular stacking interactions may be neglected, the mean decay time values (Fig. 2a) are higher than that for any dinucleotides, where base–base intramolecular stacking interactions led to dynamical quenching reflected by faster fluorescence decays. In addition, fluorescence decays of dinucleotides remarkably depend on the number of phosphates in the 5′-5′ polyphosphate bridge, and resulted values of the mean decay lifetime (Fig. 2a) and parameter of heterogeneity (Fig. 2b) are generally lowest for m^3Bp_3G. These data show that base–base intramolecular stacking interactions are strongest in m^3Bp_3G, and reflected by high dynamical quenching of m^3Bp_3G fluorescence. It seems that dynamical quenching may be weaker when polyphosphate bridge is too short or too long, as observed for m^3Bp_2G and m^3Bp_4G, respectively.

As expected, increasing temperature generally led to decrease of the mean decay time values (Fig. 2a) of m^3B fluorescence of both m^3BTP and dinucleotides. This effect is higher for dinucleotides than mononucleotide, and

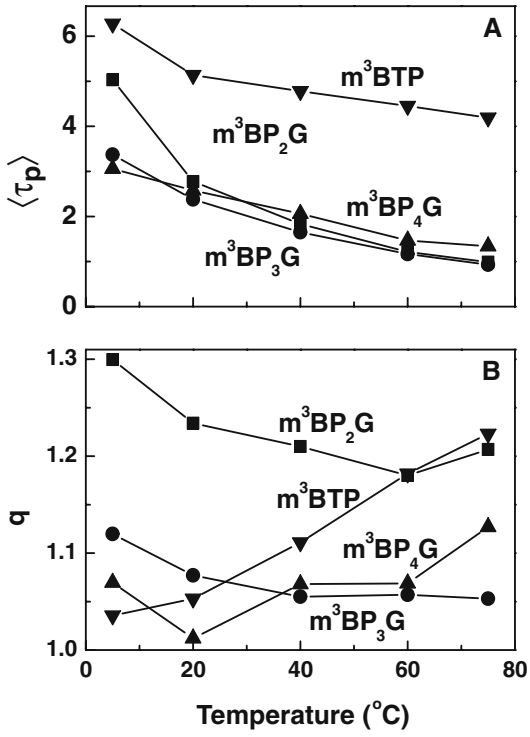

Fig. 2 Temperature dependence of **a** the mean decay time $\langle\tau_p\rangle$ and **b** the parameter of heterogeneity q obtained using power-like function (Eq. 2) fitted to the fluorescence intensity decays of 5 μM m^3BTP, m^3Bp_2G, m^3Bp_3G and m^3Bp_4G in aqueous solution. Estimated relative standard deviations ±1 and ±1.5% for q and $\langle\tau_p\rangle$, respectively. For m^3BTP (5 and 20°C) and m^3Bp_3G (75°C), the q and $\langle\tau_p\rangle$ values were somewhat at lower accuracy ±1.5 and ±2%, respectively

consistent with the fact that fluorescence quenching in dinucleotides is caused by intramolecular base–base stacking interaction. Concomitantly, the parameter of heterogeneity q decreased for each dinucleotide (Fig. 2b), and reached plateau level above 40°C, where q is lowest (N is highest) for m^3Bp_3G (Fig. 2b). In contrast, the q value for m^3BTP monotonically increases with increasing temperature (Fig. 2b), and together with temperature dependence of the mean decay time of its fluorescence reflects an intermolecular collisional quenching leading to an increase of radiationless deactivation.

All the foregoing discussions add confidence to the dominant role of intramolecular base–base stacking interaction of dinucleotides in m^3B fluorescence quenching. The lowest values of $\langle\tau_p\rangle$ and q (highest value of N) suggest that intramolecular stacking is strongest in m^3Bp_3G, and may be accounted for higher rate of fluorescence quenching.

Conclusions

New method based on the continuous lifetime distribution was applied to analysis of very complex fluorescence intensity decays of dinucleotide cap-analogues in aqueous solutions. Instead of multi-exponential function containing temperature-dependent number of components,

the physical meaning of which was unknown (Wieczorek et al. 1997), fluorescence decays were successfully fitted by physically justified two-parameter power-like function (Eq. 2). These led to values of mean decay time and heterogeneity parameter related to the mean value of lifetime distribution (Eq. 4) and relative variance (Eq. 3), respectively. Additionally, the number of decay path may be derived from the latter (Eq. 3). These parameters enable interpretation of the effect of base–base stacking interaction on the fluorescence decay heterogeneity. Increase of temperature and the length of 5′,5′-phosphate bridge in the cap affected fluorescence decay of m^3B moiety in dinucleotides, and showed that stacking interactions are strongest in the case of dinucleotide containing triphosphate chain (m^3Bp_3G). The longer or shorter 5′,5′-phosphate chain led to weaker stacking interaction. The differences in strength of stacking may arise not only from the length of the 5′,5′-phosphate bridges, but also from the value of negative charge on the phosphate chain, which is proportional to the number of phosphate groups (Scheme 1).

These observations are important for explanation of molecular mechanism of functions of the 5′-cap (Furuichi and Shatkin 2000), which serves as a site of recognition for numerous proteins involved in splicing of mRNA precursors (pre-mRNA), transport and translation of mRNA, and protects mRNA against nucleolytic degradation. The natural cap structures consist of m^7G linked by a 5′-5′ triphosphate bridge to the first transcribed nucleoside in the mRNA sequence. In spite of the different nucleosides present at this position, cap structures are recognized and bound by the same protein factors, e.g. eIF4E. We show here that the tripolyphosphate bridge is optimal for strongest stacking interactions between adjacent base moieties, which is confirmed by lowest values of both fluorescence mean decay time and relative variance of lifetime distribution. Furthermore, fluorescence studies on binding of various dinucleotide cap-analogues by eIF4E showed that triphosphate chain is also optimal for binding, and binding is stronger at elevated temperature (Niedzwiecka et al. 2002; Carberry et al. 1989), when transition to unstacked structure is easier. This may reflect some influence of the phosphate-chain length and influence of the intramolecular base–base stacking. Our observations are in line with those pointing to the importance of dynamic equilibrium between stacked and unstacked forms of caps for complex formation with eIF4E. The importance of this is also underlined by the fact that a crucial step in complex formation with the eIF4E protein is an exchange of base–base stacking in free cap into sandwich-type stacking interactions (Marcotrigiano et al. 1997; Tomoo et al. 2003) between the positively charged m^7G moiety of the cap and indole residues of two tryptophans (Trp56/m^7G/Trp102) in the cap-eIF4E complex. Note, in particular, the interaction only with the cationic form of m^7G, reflecting selectivity in the translation initiation, and lending added confidence to the validity of the chemically fixed cationic form of m^3B in m^3Bp_nG ($n = 2$, 3 and 4) dinucleotides as a model of the mRNA cap. The latter may also be used in future studies of the cation-π sandwich stacking with Trp56 and Trp102. This interaction has a high effect on the stability of the cap-eIF4E complex (Ruszczynska et al. 2003) due to electrostatic attraction between the cation of the m^7G base moiety and the quadrupole charge distribution of both indole residues. Such interaction is widely observed in protein–ligand systems (Biot et al. 2002; Gallivan and Daugherty 1999; Daugherty 1996).

Secondary stacked structure at the 5′-non-coding region of mRNA, which contains the m^7G-cap, generally inhibits translation, and is recognized as an important structural feature of mRNAs for regulating translation in eukaryota (Kozak 2005). The initiation of protein synthesis starts from interaction with protein initiation factors, e.g. with eIF4F, which are involved in melting of this secondary structure (Sonenberg 1988). Bearing in mind that transition between stacked and unstacked states of the cap analogues occurs by conformational changes (Wieczorek et al. 1997), our fluorescence studies on the m^3B cap may help to understand the importance of the length of tripolyphosphate bridge between nucleosides for overall stability of stacked cap structure, and for biological role of the latter.

Results of present studies may also help to elucidate the role of stacking interactions for the biological role of other dinucleotide polyphosphates (Np_nN, $n = 4$, 5, 6), which are found in both procatyotic and eukaryotic cells. For example, Ap_4A which is involved in the initiation of DNA replication and cell divisions (Zemecnik 1983), also exhibited structure similar to that of cap.

As a final remark we wish to emphasize that the power law function proposed here for analysis of fluorescence decay of dinucleotides is a manifestation of Tsallis non-extensive statistics (Tsallis 1988). In this approach (Tsallis 1988) a power-like formula (q-exponential function),

$$\left[1-(1-q)\frac{t}{\tau}\right]^{1/(1-q)} \underset{q\to 1}{\rightarrow} \exp\left(-\frac{t}{\tau}\right)$$

is a generalization of the classical Boltzmann–Gibbs function, replaces the usual exponential function, and reproduces it for $q \rightarrow 1$. Power-like function is determined only by two parameters, and, hence, is advantageous for multi-exponential functions by increased efficiency of fitting. It is suitable for description of a variety of systems, ranging from econophysics to cosmology, characterized by long-range correlations, long-range microscopic memories or fluctuations of some parameters of the system. These fluctuations may affect fluorescence decay in oligonucleotides, and lead to fluorescence lifetime distribution and power-like decay, as was observed for the dinucleotide cap-analogues.

Acknowledgements We are grateful to Dr. Lidia Chlebicka and Dr. Edward Darzynkiewicz (Department of Biophysics, Warsaw University) for the availability of methylbenzimidazole analogues. This investigation was supported by the Polish Ministry of Scientific

Research and Information Technology (MNiI), grants no. 1P03B11128, and partially by 3P04A02425, BW-1605/BF and BST 975/BF.

References

Biot C, Buisine E, Kwasigroch J-M, Wintjens R, Rooman M (2002) Probing the energetic and structural role of amino acid/nucleobase cation-π interactions in protein–ligand complexes. J Biol Chem 277:40816–40822

Blachut-Okrasinska E, Bojarska E, Niedzwiecka A, Chlebicka L, Darzynkiewicz E, Stolarski R, Stepinski J, Antosiewicz JM (2000) Stopped-flow and Brownian dynamics studies of electrostatic effects in the kinetics of binding of 7-methyl-GpppG to the protein eIF4E. Eur Biophys J 29:487–498

Brooks BR, Bruccoleri RE, Olafson BD, States DJ, Swaminathan S, Karplus M (1983) CHARMM: a program for macromolecular energy minimization and dynamics calculations. J Comput Chem 4:187–215

Carberry SE, Rhoads RE, Goss DJ (1989) A spectroscopic study of the binding of m^7GTP and m^7GpppG to human protein synthesis initiation factor 4E. Biochemistry 28:8078–8083

Chlebicka L, Wieczorek Z, Stolarski R, Stępiński J, Darzynkiewicz E, Shugar D (1995) Synthesis and properties of mRNA 5′-cap analogues with 7-methylguanine replaced by benzimidazole or 3-methylbenzimidazol. Nucleos Nucleot 14:771–775

Daugherty DA (1996) Cation-π interactions in chemistry and biology: a new view of benzene, Phe, Tyr, and Trp. Science 271:163–168

Długosz M, Wlodarczyk J (2004) The relationship between the kinetics of the excitation transport and the structure of an organic model compound by means of molecular dynamics and luminescence decay function analysis. In: Summer School on Advanced Modelling of Biological Function, Bremen, Germany

Dlugosz M, Blachut-Okrasinska E, Bojarska E, Darzynkiewicz E, Antosiewicz JM (2003) Effects of pH on kinetics of binding of mRNA-cap analogs by translation initiation factor eIF4E. Eur Biophys J 31:608–616

Furuichi F, Shatkin AJ (2000) Viral and cellular mRNA capping: past and prospects. Adv Virus Res 55:135–184

Gallivan JP, Dougherty DA (1999) Cation-π interactions in structural biology. Proc Natl Acad Sci USA 96:9459–9464

Hu G, Tsai A-L, Quiocho FA (2003) Insertion of an N7-methylguanine mRNA cap between two coplanar aromatic residues of a cap-binding protein is fast and selective for a positively charged cap. J Biol Chem 51:51515–51520

Jean JM, Hall KB (2004) Stacking–unstacking dynamics of oligodeoxynucleotide trimers. Biochemistry 43:10277–10284

Kozak M (2005) Regulation of translation via mRNA structure in prokaryotes and eukaryotes. Gene 361:13–37

Larsen OFA, van Stokkum IHM, de Weerd FL, Vengris M, Aravindakumar CT, van Grondelle R, Geacintov NE, van Amerongen H (2004) Ultrafast transient-absorption and steady-state fluorescence measurements on 2-aminopurine substituted dinucleotides and 2-aminopurine substituted DNA duplexes. Phys Chem Chem Phys 6:154–160

Levenberg KA (1944) A method for the solution of certain nonlinear problems in least squares. Quart Appl Math II(2):164–168

Marcotrigiano J, Gingras AC, Sonnenberg N, Burley SK (1997) Cocrystal structure of the messenger RNA 5′ cap-binding protein (eIF4E) bound to 7-methyl-GDP. Cell 89:951–961

Marquardt DW (1963) An algorithm for least-squares estimation of nonlinear parameters. J Soc Ind Appl Math 11:431–441

Mathews MB, Sonenberg N, Hershey JWB (2000) Origins and principles of translation control. In: Sonenberg N, Hershey JWB, Mathews MB (eds) Translational control of gene expression. Cold Spring Harbor Laboratory Press, Plainview, New York, pp 1–32

Niedzwiecka A, Marcotrigiano J, Stepinski J, Jankowska-Anyszka M, Wyslouch-Cieszynska A, Dadlez M, Gingras A-C, Mak P, Darzynkiewicz E, Sonnenberg N, Burley SK, Stolarski R (2002) Biophysical studies of eIF4E cap-binding protein: recognition of mRNA 5′ cap structure and synthetic fragments of eIF4G and 4E-BP1 proteins. J Mol Biol 319:615–635

Nishimura Y, Takahashi S, Yamamoto T, Tsuboi M, Hattori M, Miura K, Yamaguchi K, Ohtani S, Hata T (1980) On the base-stacking in the 5′-terminal cap structure of mRNA: a fluorescence study. Nucleic Acids Res 8:1107–1119

O'Neill MA, Barton JK (2004) DNA charge transport: conformationally gated hopping through stacked domains. J Am Chem Soc 126:11471–11483

O'Neill MA, Becker HC, Wan C, Barton JK, Zewail AH (2003a) Ultrafast Dynamics in DNA-mediated electron transfer: base gating and the role of temperature. Angew Chem 47:6076–6080

O'Neill MA, Becker HC, Wan C, Barton JK, Zewail AH (2003b) Ultrafast dynamics in DNA mediated electron transfer: base gating and the role of temperature. Angew Chem Int Ed 42:5896–5900

Ruszczynska R, Kamienska-Trela K, Wojcik J, Stepinski J, Darzynkiewicz E, Stolarski R (2003) Charge distribution in 7-methylguanine regarding cation-π interaction with protein factor eIF4E. Biophys J 85:1450–1456

Saenger W (1984) Principles of nucleic acids structure. Springer, Berlin Heidelberg New York

Sonenberg N (1988) Cap-binding proteins of eukaryotic messenger RNA: functions in initiation and control of translation. Prog Nucleic Acid Res Mol Biol 35:173–207

Stolarski R, Zdanowski K, Chlebicka L, Wieczorek Z, Sitek A, Stepinski J, Jankowska M, Mattinen J, Temeriusz A, Darzynkiewicz E (1996) Inter- and intramolecular stacking of mRNA cap-analogues—relevance to initiation of translation. Collect Czech Chem Commun 61(special issue):217–221

Stoychev G, Kierdaszuk B, Shugar D (2001) Interaction of *Escherichia coli* purine nucleoside phosphorylase (PNP) with the cationic and zwitterionic forms of the fluorescent substrate N(7)-methylguanosine. Biochim Biophys Acta 1544:74–88

Su T-J, Connolly BA, Darlington C, Mallin R, Dryden DTF (2004) Unusual 2-aminopurine fluorescence from a complex of DNA and the EcoKI methyltransferase. Nucleic Acids Res 32:2223–2230

Tomoo K, Shen X, Okabe K, Nozoe Y, Fukuhara S, Morino S, Ishida T, Taniguchi T, Hasegawa H, Terashima A, Sasaki M, Katsuya Y, Kitamura K, Miyoshi H, Ishikawa M, Miura K (2002) Crystal structures of 7-methylguanosine 5′-triphosphate (m(7)GTP)- and P(1)-7-methylguanosine-P(3)-adenosine-5′,5′-triphosphate (m(7)GpppA)-bound human full-length eukaryotic initiation factor 4E: biological importance of the C-terminal flexible region. Biochem J 362:539–544

Tomoo K, Shen X, Okabe K, Nozoe Y, Fukuhara S, Morino S, Sasaki M, Taniguchi T, Miyagawa H, Kitamura K, Miura K, Ishida T (2003) Structural features of human initiation factor 4E, studied by X-ray crystal analyses and molecular dynamics simulations. J Mol Biol 328:365–383

Tsallis C (1988) Possible generalization of Boltzmann–Gibbs statistics. J Stat Phys 52:479–487; For updated bibliography on this subject see http://www.tsallis.cat.cbpf.br/biblio.htm; cf. also special issue of Braz J Phys 29 (1999) available at http://www.sbf.if.usp.br/bjp/Vol29/Num1/index.htm

Wieczorek Z, Zdanowski K, Chlebicka L, Stepinski J, Jankowska M, Kierdaszuk B, Temeriusz A, Darzynkiewicz E, Stolarski R (1997) Fluorescence and NMR studies of intramolecular stacking of mRNA cap-analogues. Biochim Biophys Acta 1354:145–152

Wilk G, Włodarczyk Z (1999) Interpretation of the nonextensivity parameter q in some applications of Tsallis statistics and Lévy distributions. Phys Rev Lett 84:2770–2773

Wlodarczyk J, Kierdaszuk B (2003) Interpretation of fluorescence decays using a power-like model. Biophys J 85:589–598

Wlodarczyk J, Kierdaszuk B (2005) Fluorescence decay heterogeneity model based on electron transfer processes in an enzyme-ligand complex. Acta Phys Pol A 107:883–894

Zemecnik P (1983) Diadenosine 5′,5-P^1, P^4 -tetraphosphate (Ap_4A): its role in cellular metabolism. Anal Biochem 134:1–10